Optimum Threshold Parameter Estimation of Bidimensional Empirical Mode Decomposition Using Fisher Discriminant Analysis for Speckle Noise Reduction

Mohammad-Motiur Rahman[1], Mithun-Kumar Pk[1], and Mohammad-Shorif Uddin[2]
[1]Department of Computer Science and Engineering, Mawlana Bhashani Science and Technology University, Bangladesh
[2]Department of Computer Science and Engineering, Jahangirnagar University, Bangladesh

Abstract: *Now a days Empirical Mode Decomposition (EMD) is an important tool for image analyzing. Optimizing threshold value of Bidimensional Intrinsic Mode Function (BIMF) is one of the important tasks in speckle noise reduction in the Bidimensional Empirical Mode Decomposition (BEMD) domain. Without proper selection of threshold value image information may be lost, which is unwanted. In this paper we proposed optimum threshold parameter using Fisher Discriminant Analysis (FDA) for determining the optimum threshold value of the Intrinsic Mode Functions (IMF) for the best speckle noise reduction. In the mean time, we used the optimal threshold value for separating the higher frequency signal from BIMF to calculate the mean of these separated signals for alleviating speckle noise. It also preserves edges without loss of important image information. The method is compared with the several other classical thresholding methods on variety of images and the experimental results confirm significant improvement over existing methods.*

Keywords: *EMD, BEMD, FDA, IMF, BIMF, optimum threshold, speckle noise, ultrasound image.*

Received August 25, 2013; accepted March 20, 2014; published online September 4, 2014

1. Introduction

For image preprocessing denoising is one of the most vital and important tasks. The aim of the image denoising algorithm is to reduce the noise level as well as preserving the important image features or information. Speckle is a particular kind of multiplicative noise which occurs in images obtained by coherent imaging systems like ultrasound. It tends to degrade the resolution and contrast of ultrasound images, thus may lead to eliminate some useful and important diagnostic information. In the recent years there has been a fair amount of research on wavelet thresholding for signal denoising because wavelet provides appropriate basis for separating noise signal from image signal. The main challenge of this method is to find an optimum threshold value because a small threshold value will pass all the noisy coefficients and hence, the resultant denoised signal may still be noisy. On the other hand, a large threshold value makes more number of coefficients as zero which leads to smooth signal and destroys details and image may produce blur and artifacts. Many wavelet based thresholding techniques like hard thresholding, soft thresholding, VisuShrink, SureShrink, BayesShrink and Bayes thresholding [1, 5, 6, 7, 8, 9, 10, 11, 13, 15, 19, 22] have proved better efficiency in image processing. Bayes thresholding is selected by maximum likelihood estimation.

Empirical Mode Decomposition (EMD) is a relatively new signal processing method that was originally designed to analyze nonlinear and non-stationary One-Dimensional (1D) signals [12]. Bidimensional Empirical Mode Decomposition (BEMD) is a Two-Dimensional (2D) extension of the concept of EMD, which is a multi-resolution decomposition technique aimed mainly for image processing [4, 14, 16]. BEMD and its variants decompose an image into several Bidimensional Intrinsic Mode Functions (BIMFs) and a Bidimensional Residue (BR). BEMD is a very efficient method for extracting the higher frequency part BIMF of the images in order to alleviate noise using several types of filters and the state-of-art algorithms.

Fisher Discriminant Analysis (FDA) [2] has been widely applied in pattern recognition and classification. Fthat it is sometime necessary for finding threshold value. In papers [2, 21] FDA is used for selecting optimum threshold value for pattern recognition and classification. In [24] wavelet based denoising preprocessing with FDA scheme is proposed for fault diagnosis. In this paper we proposed FDA based thresholding method for denoising speckle noise of different images. Figure 1 shows a simple flow diagram of our system. This paper is the improve version of our previous research work [18] and this paper shows better performance than [18].

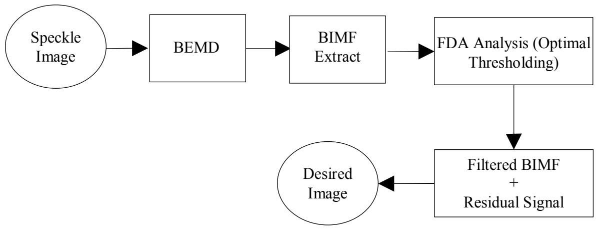

Figure 1. Block diagram of the proposed FDA technique for accurate speckle noise reduction and the best edge preservation approach for ultrasound image.

The paper is organized as follows: In section 2, we define the ultrasound speckle suppression problem by outlining the speckle noise model and the fisher discriminant analysis. Section 3 describes some existing thresholding methodology. Section 4 depicts EMD and Intrinsic Mode Functions (IMF) extraction. Section 5 the numerical implementation scheme of the proposed FDA optimal threshold method is presented. Section 6 presents the evaluation criteria for checking the filter performance. Section 7 compares the performance of the proposed method with other existing speckle noise reduction methods.

2. Theoretical Background

2.1. Speckle Noise Model

Denote by a noisy observation $I(x, y)$ (i.e., the recorded ultrasound image) of the 2D function $f(x, y)$ (i.e., the noise-free image that has to be recovered) and by $\eta_{m(x, y)}$ and $\eta_{a(x, y)}$ the corrupting multiplicative and additive speckle noise components, respectively. One can write:

$$I(x, y) = f(x, y)\cdot \eta_m(x, y) + \eta_a(x, y) \tag{1}$$

Generally, the effect of the additive component of the speckle in ultrasound images is less significant than the effect of the multiplicative component. Thus, ignoring the term $\eta_a(x, y)$, one can rewrite Equation 1 as:

$$I(x, y) = f(x, y)\cdot \eta_m(x, y) \tag{2}$$

To transform the multiplicative noise model into an additive one, we apply the logarithmic function on both sides of Equation 2.

2.2. Fisher Discriminant Analysis

FDA locates directions efficient for discrimination by yielding the maximum ratio of between-class scatter to within-class scatter. For each image fisher linear discriminant finds a projection orientation of intensity by which two classes (object and background) are well separated. For any image, there is a set X including N intensity.

$$\begin{gathered} X = \{C_1, C_2\} = \{x_1, x_2, \ldots, x_n\} \\ n_1 + n_2 = N \end{gathered} \tag{3}$$

Where n_1 and n_2 are cardinality of subset C_1 and subset C_2 respectively. If we form a linear combination of the components of x_i. We obtain:

$$y_i = W^T x_i \tag{4}$$

Of all the possible lines we would like to select the one that maximizes the separability of the scalars. In order to, find a good projection vector, we need to define a measure of separation. The mean vector of each class in x space and y space is:

$$\mu_i = \frac{1}{N_i} \sum_{x \in \omega_i} x \tag{5}$$

And

$$\tilde{\mu}_i = \frac{1}{N_i}\sum_{y \in \omega_i} y = \frac{1}{N_i}\sum_{x \in \omega_i} W^T x = W^T \mu_i \tag{6}$$

We can then choose the distance between the projected means as our objective function:

$$J(W) = \left|\tilde{\mu}_1 - \tilde{\mu}_2\right| = \left|W^T(\mu_1 - \mu_2)\right| \tag{7}$$

However, the distance between projected means is not a good measure since it does not account for the standard deviation within classes. Fisher suggested maximizing the difference between the means, normalized by a measure of the within-class scatter. For each class we define the scatter, an equivalent of the variance, as:

$$\tilde{s}_i^2 = \sum_{y \in \omega_i} (y - \tilde{\mu}_i)^2 \tag{8}$$

Where the quantity $(\tilde{S}_1^2 + \tilde{S}_2^2)$ is called the within-class scatter of the projected examples. The fisher linear discriminant is defined as the linear function $W^T x$ that maximizes the criterion function.

$$J(W) = \frac{\left|\tilde{\mu}_1 - \tilde{\mu}_2\right|^2}{\tilde{S}_1^2 + \tilde{S}_2^2} \tag{9}$$

Therefore, we are looking for a projection examples from the same class are projected very close to each other and at the same time, the projected means are as farther apart as possible. To find the optimum W, first we define a measure of the scatter in feature space x.

$$s_i = \sum_{x \in \omega_i} (x - \mu_i)(x - \mu_i)^T \tag{10}$$

$$S_1 + S_2 = S_W \tag{11}$$

Where S_W is called the wit in class scatter matrix. The scatter of the projection y can then be expressed as a function of the scatter matrix in feature space x.

$$\begin{aligned} \tilde{s}_i^2 &= \sum_{y \in \omega_i} (y - \tilde{\mu}_i)^2 = \sum_{x \in \omega_i} (W^T x - W^T \mu_i)^2 \\ &= \sum_{x \in \omega_i} W^T (x - \mu_i)(x - \mu_i)^T W = W^T S_i W \end{aligned} \tag{12}$$

$$\tilde{S}_1^2 + \tilde{S}_2^2 = W^T S_W W \tag{13}$$

Similarly, the difference between the projected means can be expressed in terms of the means in the original feature space.

$$(\tilde{\mu}_1 - \tilde{\mu}_2)^2 = (W^T \mu_1 - W^T \mu_2)^2 = W^T (\mu_1 - \mu_2)(\mu_1 - \mu_2)^T W = W^T S_B W \tag{14}$$

The matrix S_B is called the between class scatter. Note that, since S_B is the outer product of two vectors, its rank is at most one. We can finally express the fisher criterion in terms of S_W and S_B as:

$$J(W)=\frac{W^T S_B W}{W^T S_W W} \tag{15}$$

To find the maximum of $J(W)$ we derive and equate to zero.

$$\frac{d}{dw}[J(W)]=\frac{d}{dw}\left[\frac{W^T S_B W}{W^T S_W W}\right]=0\Rightarrow\left[W^T S_W W\right]\frac{d\left[W^T S_B W\right]}{dw} -\left[W^T S_B W\right]\frac{d\left[W^T S_W W\right]}{dw}=0\Rightarrow \tag{16}$$

Dividing by $W^T S_W W$:

$$\left[\frac{W^T S_W W}{W^T S_W W}\right]S_B W-\left[\frac{W^T S_B W}{W^T S_W W}\right]S_W W=0$$
$$\Rightarrow S_B W - J S_W W=0 \Rightarrow S_W^{-1} S_B W - JW=0 \tag{17}$$

Solving the generalized eigen value problem yields $S_W^{-1} S_B W = JW$.

$$W^* = \arg\max\left[\frac{W^T S_B W}{W^T S_W W}\right]= S_W^{-1}(\mu_1-\mu_2) \tag{18}$$

This is knows as Fisher's Linear Discriminant (FLD).

3. Thresholding Methodology

3.1. Wavelet Shrinkage

Let $W(0)$ and $W^1(0)$ denote the forward and inverse wavelet transform operators. Let $D(0, \lambda)$ denote the thresholding operator with threshold λ . The practice of thresholding denoising consists of the following three steps:

- *Step* 1: $Y=W(x)$.
- *Step* 2: $Z=D(Y, \lambda)$.
- *Step* 3: $\hat{x}= W^1(Z)$.

Hard thresholding and soft thresholding are only different in step 2.

3.1.1. Hard Thresholding

In the case of hard thresholding:

$$D(Y, \lambda)=\begin{cases} Y & if \|Y\|>\lambda \\ 0 & otherwise \end{cases} \tag{19}$$

3.1.2. Soft Thresholding

In the case of soft thresholding or Wavelet shrinkage:

$$D(Y, \lambda)=\begin{cases} sign(Y)(\|Y\|-\lambda) & if \|Y\|>\lambda \\ 0 & otherwise \end{cases} \tag{20}$$

3.2. BayesShrink

The observation model is $Y=X+V$, with X and V independent of each other, hence:

$$\sigma_Y^2=\sigma_X^2+\sigma^2 \tag{21}$$

Where the noise variance σ^2 is estimated from the subband $HH1$ by the robust median estimator [20]:

$$\sigma=\frac{Median(|Y_{ij}|)}{0.6745},\quad Y_{ij}\in subband\ HH_1 \tag{22}$$

And σ_Y^2 is the variance of Y. Since, Y is modeled as zero-mean, σ_Y^2 can be found empirically by:

$$\hat{\sigma}_Y^2=\frac{1}{n}\sum_{i,j=1}^{n} Y_{ij}^2 \tag{23}$$

Where $n\times n$ is the size of the subband under consideration. Thus:

$$\hat{T}_B(\hat{\sigma}_X)=\frac{\hat{\sigma}^2}{\hat{\sigma}_X} \tag{24}$$

Where $\hat{\sigma}_X=\sqrt{max(\hat{\sigma}_Y^2-\hat{\sigma}^2, 0)}$.

4. Empirical Mode Decomposition

The EMD is a relatively new method for analyzing and processing non-stationary, non-linear signals [3]. The EMD reduces a time signal into a set of basis signals just like of the fourier or wavelet transforms; unlike the fourier or wavelet transforms, however, the basis functions are derived from the data itself. Each basis function of the EMD is known as an IMF, captures the repeating behavior of the signal at some particular time scale.

4.1. EMD Principle

The decomposition has an assumption that any data consists of different simple intrinsic models of oscillations. Each intrinsic mode, no matter linear or not, represents an oscillation, which will have the same number of extrema and zero-crossings and then the oscillation will be symmetric with respect to the local mean. Usually, the data may have many different oscillations which can be represented by the IMF with following definition:

a. In the whole dataset, the number of extrema and the number of zero-crossings must either equal or differ at most by one.
b. At any point, the mean value of the envelope defined by the local maxima and the envelope defined by the local minima is zero. An IMF is much more general than an oscillation mode because it has a variable amplitude and frequency as a function of time. According to the definition for the IMF, we can decompose any function as follows [23] and Figure 2 as an example.

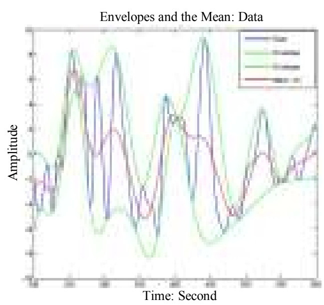

Figure 2. The mean value of the envelope is estimated by the local maxima and the local minima.

4.2. IMF Extraction Procedure

IMF is the main part of EMD for making separation higher frequency from signals. IMF extraction procedure follows:

1. First, find all the local maxima extrema of $x(t)$.
2. Interpolate (cubic spline fitting) between all the maxima extrema ending up with some upper envelope $e_{max}(t)$.
3. Find all the local minima extrema.
4. Interpolate (cubic spline fitting) between all the minima extrema ending up with some lower envelope $e_{min}(t)$.
5. Compute the mean envelope between upper envelope and lower envelope.

$$m(t)=\frac{e_{min}(t)+e_{max}(t)}{2} \tag{25}$$

6. Extract the higher frequency as an IMF function from the signal:

$$d(t)=x(t)-m(t) \tag{26}$$

7. IMF extraction flow:

$$\begin{aligned} x(t) &= d_1(t)+r_1(t) \\ &= d_1(t)+d_2(t)+r_2(t) \\ &\vdots \\ &= \sum_{i=1}^{K} d_i(t)+r_K(t) \end{aligned} \tag{27}$$

Where $d_1(t)$ high frequency part IMF and $r_K(t)$ stands for residual trend (a low order polynomial component) and iterate on the slow oscillations component considered as a new signal. So:

$$r_1(t)=d_2(t)+r_2(t) \tag{28}$$

5. Proposed Method

5.1. Objective Function

Firstly, BEMD is applied on an image for creating the BIMF. An image is $f(x, y)$ and the size of image is $M\times N$ then, BIMF $d(x, y)$ will be generated by this procedure:

$$\begin{aligned} f(x,y) &= d_1(x,y)+r_1(x,y) \\ &= d_1(x,y)+d_2(x,y)+r_2(x,y) \\ &\vdots \\ &= \sum_{i=1}^{K} d_i(x,y)+r_K(x,y) \end{aligned} \tag{29}$$

Where K=10 that means we extract 10 levels BIMF coefficients. Individually each coefficient is denoted by n_i. Total number of coefficient $N=n_0+n_1+n_2+ \ldots +n_M$. Now, we have to calculate each coefficient probability using below this Equation:

$$P_i=\frac{n_i}{N}; \quad P_i \geq 0 \tag{30}$$

Where $\sum_{i=0}^{M} P_i=1$.

Suppose that, the coefficients are divided into two classes C_1 and C_2 by a fixed value t; C_1 is the set of coefficients with levels [0, 1, ..., L] and the rest of coefficients belong to C_2 C_1 and C_2 normally correspond to the object class and the back ground one, or vice versa. Then, the probabilities of the two classes are given by within:

$$W_1(L)=\sum_{i=0}^{L} P_i \tag{31}$$

$$W_1(L)=1-W_1(L) \tag{32}$$

The mean coefficients of the two classes can be defined as:

$$\mu_1=\sum_{i=0}^{L}\frac{iP_i}{W_1} \tag{33}$$

$$\mu_2=\sum_{i=L+1}^{M}\frac{iP_i}{W_2} \tag{34}$$

Corresponding class variances are given by:

$$\sigma_1^2=\sum_{i=0}^{L}\frac{(i-\mu_1)^2 P_i}{W_1} \tag{35}$$

$$\sigma_2^2=\sum_{i=L+1}^{M}\frac{(i-\mu_2)^2 P_i}{W_2} \tag{36}$$

The within-class variance can be defined [17]:

$$\sigma_W^2=W_1\sigma_1^2+W_2\sigma_2^2 \tag{37}$$

As we have seen in section 2.2, the FLD seeks directions efficient for discrimination by yielding the maximum ratio of between class scatter to within class scatter. Thus, based on the function defined by Equation 9 the following criterion as objective function to evaluate the separability of the threshold at level L.

$$\rho(L)=\frac{(\mu_1(L)-\mu_2(L))^2}{\sigma_W^2} \tag{38}$$

Where $\sigma_W^2=W_1\sigma_1^2+W_2\sigma_2^2$.

From Equation 38 we shall get FDA thresholding value T between two classes as follows. T can be used for separating two classes but, if we want to apply threshold value T for noise reduction then this type of thresholding can not be efficient for noise reduction. These situations we can overcome by applying the standard deviation and mean value ratio of the coefficient of any IMF of EMD. Here, we proposed the proper threshold value estimation method for speckle noise reduction in the EMD domain. So, this method is given below:

If the BIMF is $\xi(x, y)$ and the size is $F\times H$ then the mean value of BIMF is:

$$\mu_c=\frac{1}{F\times H}\sum\xi(x,y) \tag{39}$$

And the standard deviation of the BIMF coefficient is:

$$\sigma_c=\sqrt{\frac{\sum_{x=0}^{F-1}\sum_{y=0}^{H-1}[\xi(x,y)-\mu_c]^2}{F\times H}} \tag{40}$$

For the large FDA threshold value T huge amount of diagnostic information is lost. To remove this limitation we use mathematical operations between mean and standard deviation of BIMF coefficients with respect to FDA threshold value to obtain an optimal threshold value. The proposed optimal threshold value is:

$$T_{optimal} = \frac{T}{\sqrt{\left|\frac{\sigma_c}{\mu_c}\right|}} \quad (41)$$

Where $\left|\frac{\sigma_c}{\mu_c}\right| > 0$.

Now, we get optimal threshold value from Equation 41 using FDA for speckle noise reduction of ultrasound images. We know $\xi(x, y)$ is the BIMF coefficient and optimal threshold value is $T_{optimal}$. *Optimal* threshold operation on BIMF coefficients is shown below:

```
for(x=1 to F)
{
   for(y=1 to H)
      {
         if (ξ[x, y] ≥ T_optimal)
           { H_c[x, y]=ξ[x, y];}
      }
}
```

Calculate the mean value of $H_c[x, y]$ is M. Then $H_c[x, y]=M$

We use "Lena" image for testing the performance between FDA thresholding and FDA optimal thresholding. From Table 1 we see that FDA optimal thresholding exhibits better performance than FDA thresholding. Here, we show the histogram comparison and efficiency of those threshold values as shown in Figure 3.

From Figure 3, we see that Figure 3-b lost its structural view but Figures 3-c and d have a structural view without loss of important information with respect to original image and 3-d is better than 3-c. We observe that FDA *optimal* threshold show the better performance for edge preservation over existing FDA threshold. Very small amount of error occurred in the filtered image for FDA *optimal* thresholding technique and enhance the image clearly. From these measurements, we can realize that FDA *optimal* threshold performance significantly better than FDA threshold.

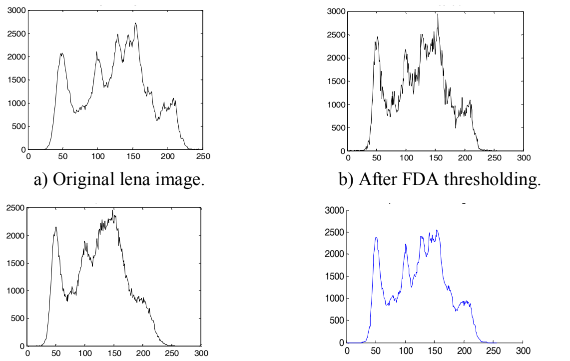
a) Original lena image. b) After FDA thresholding. c) After FDA optimal thresholding with wavelet. d) After FDA optimal thresholding with BEMD.

Figure 3. Histogram of Lena image with FDA thresholding operation.

5.2. Proposed Denoising Algorithm

Following steps describe the proposed algorithm for image denoising:

1. Let max_ρ=0, be the maximum value of the objective function.
2. For k=0 to Maximum of coefficient value.
3. Compute the objective function value corresponding to the coefficient value k.

   If $max_\rho < P(k)$
   then
   $max_\rho = P(k)$
   $T=k$
   end

4. The *optimal* threshold value estimation for denoising in EMD field:

   $$T_{optimal} = \frac{T}{\sqrt{\left|\frac{\sigma_c}{\mu_c}\right|}}$$

   Where $\left|\frac{\sigma_c}{\mu_c}\right| > 0$

5. BIMF coefficient is denoted by I_c and *optimal* threshold value performance is:

   If $I_c \geq T_{optimal}$
   then $H_c = I_c$,
   end

6. Compute the mean value M from the H_c.
7. Modify optimal threshold located pixels H_c by M.
8. Finally, sum up all modified BIMF with residual signals.

6. Evaluation Criteria

We observe the performance by apply Signal to Noise Ratio (SNR), Mean Square Error (MSE) and Edge Preservation Factor (EPF) parameter [20]. SNR:

$$SNR = -10 \log 10 \left[\frac{\sum_{x=1}^{M} \sum_{y=1}^{N} (I_d(x,y) - I(x,y))^2}{\sum_{x=1}^{M} \sum_{y=1}^{N} (I_d(x,y))^2} \right] \quad (42)$$

The edge preservation ability of the filter is compared by EPF and is computed using EPF:

$$EPF = \frac{\sum (\Delta I - \overline{\Delta I})(\Delta I_d - \overline{\Delta I_d})}{\sqrt{\sum (\Delta I - \overline{\Delta I})^2 (\Delta I_d - \overline{\Delta I_d})^2}} \quad (43)$$

Where ΔI and ΔI_d are the high pass filtered versions of original image I and filtered image I_d respectively, obtained with a 3×3 pixel standard approximation of the Laplacian operator. The larger value of EPF means more ability to preserve edges. MSE:

$$MSE = \left[\frac{1}{M \cdot N} \sum_{x=0}^{M-1} \sum_{y=0}^{N-1} (I(x,y) - I_d(x,y))^2 \right] \quad (44)$$

Where the image size is $M \times N$.x means row, y means column, I means original image and I_d means filtered image.

7. Experimental Result

The proposed algorithm has been applied to 2D ultrasound image with have been corrupted by multiplicative noise (speckle noise of variance 0.004). The computation is carried out on MATLAB 7.12.0.635 (R2011a) in a Core i5 2.50GHz and 4GB RAM Laptop having a Windows 7 operating system. We choose four images (e.g., Phantom, Lena, Kidney, Liver) for testing the performance of the proposed algorithm. Our proposed algorithm is compared with existing method which is shown in Tables 1 and 2 Figures 6, 7 and 8 respectively.

Table 1. For phantom and lena images.

Method	Phantom			Lena		
	SNR	EPF	MSE	SNR	EPF	MSE
Wavelet Hard Threshold	22.0213	0.1643	4.8215	22.3069	0.2273	5.8765
WaveletSoft Threshold	22.4155	0.3372	4.7151	22.8611	0.2892	5.1722
Bayesian Threshold	23.2231	0.5032	3.4014	23.8748	0.4370	4.0986
FDA Denoising with Wavelet	23.9296	0.6227	2.0191	26.5587	0.6949	2.9883
FDA Denoising with BEMD	25.8742	0.9892	1.0843	27.4771	0.9791	1.9015

Table 2. For ultrasound kidney and liver images.

	Kidney			Liver		
	SNR	EPF	MSE	SNR	EPF	MSE
Wavelet Hard Threshold	8.5828	0.2554	4.7968	14.6471	0.3443	4.9520
Wavelet Soft Threshold	8.5253	0.2532	4.8029	14.6147	0.3636	4.9625
Bayesian Threshold	8.5949	0.3471	4.5668	14.6950	0.4622	4.8874
FDA Denoising with Wavelet	11.1302	0.5934	2.7511	17.7252	0.6972	2.2166
FDA Denoising with BEMD	18.5737	0.9834	2.0615	19.6260	0.9801	1.6934

Experimental numerical results show the improved speckle noise reduction capabilities of the proposed FDA optimal threshold based filtering compared to the classical methods. From Tables 1 and 2, we see that our proposed filter effectively and properly remove speckle noise from ultrasound images because a small amount of error is occurred in the filter image and the proposed method is shown the mentionable edge preservation. We can make a decision based on the last two rows in each tables optimal threshold value is more effective and suitable for EMD rather than wavelet domains.

Histograms of original and filtered images are given below:

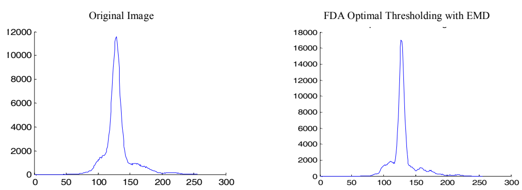

a) Phantom image.

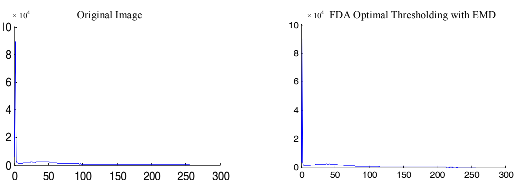

b) Kidney image.

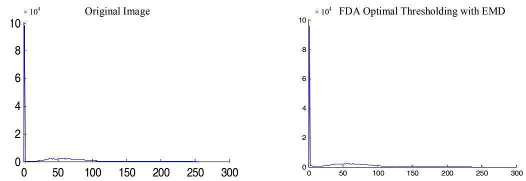

c) Liver image.

Figure 4. Histogram of the original and filtered images after FDA optimal threshold applies in images for phantom, lena, kidney, liver respectively.

Figure 4 mainly depicts the intensity variation of the images by the histograms. We observe from these histograms very small amount of the gray values are varied of the filtered images with respect to original images. So, we can easily say that a small amount of information is lost and very small amount of error is occurred in the filtered images. Naturally, filtered image is so structural that means the edge preservation and smoothness of the filtered image is really good with respect to original image.

From Figure 5 we see that Figure 5-b is an integrated higher frequency signals which is sum up 10 levels filtered BIMF and Figure 5-c is the residual image which is very low frequency signals and last one Figure 5-d is our desire image which is natural and smooth with respect to the original noisy image.

FDA optimal threshold effect on BEMD is shown below:

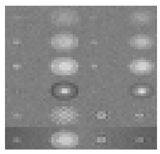

a) Phantom noisy image.

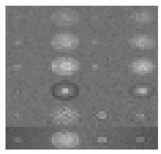

b) BIMF image.

c) Residual image.

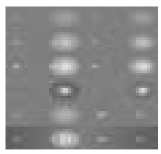

d) FDA Denoising with BEMD.

Figure 5. Mean and variance curve of diagonal coefficient of Cameraman image a and b for the first level and c and d for the second level.

From Figures 6, 7 and 8 proposed filtered image visual quality is absolutely good because our proposed algorithm shows better performance for speckle noise reduction. From the observation of the proposed filtered image, we see that it is so smooth and enhance over existing despeckle methods images and its has no any checker board and blurring effect in the homogeneous regions but preserve edges significantly without loss vital information of the image. From the visual quality we can assume that Figure 8-h is always better than Figure 8-f that means BEMD is more efficient than wavelet for extracting higher signal for speckle noise suppression.

Visual quality comparison is given below:

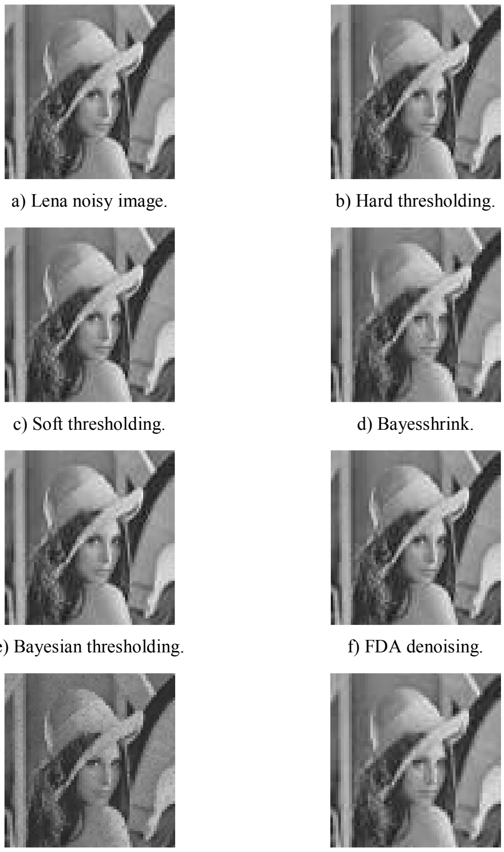

a) Lena noisy image. b) Hard thresholding.

c) Soft thresholding. d) Bayesshrink.

e) Bayesian thresholding. f) FDA denoising.

g) Filtered BIMF (10 levels). h) FDA denoising with BEMD.

Figure 6. Visual comparison of Lena image after execution some existing state-of-the-art filters and our proposed filter on Lena noisy image.

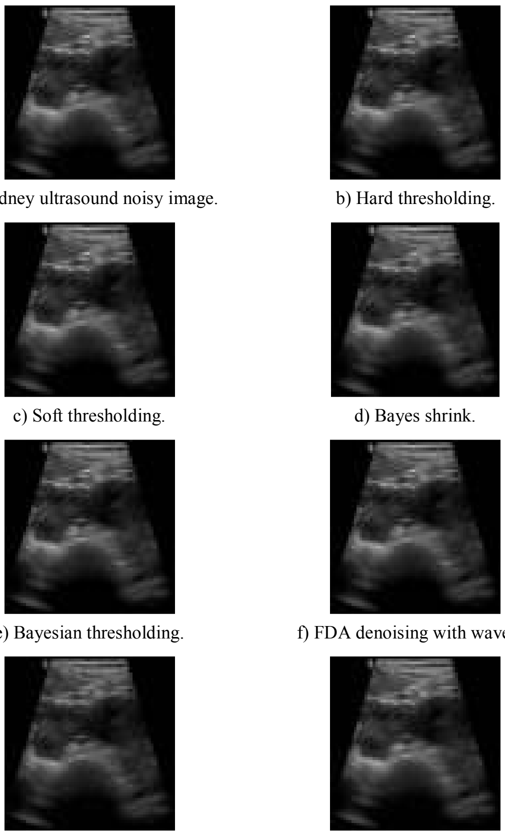

a) Kidney ultrasound noisy image. b) Hard thresholding.

c) Soft thresholding. d) Bayes shrink.

e) Bayesian thresholding. f) FDA denoising with wavelet.

g) Filtered BIMF (10 levels). h) FDA denoising with BEMD.

Figure 7. Visual comparison of kidney ultrasound image after execution some existing state-of-the-art filters and our proposed filter on kidney ultrasound noisy image.

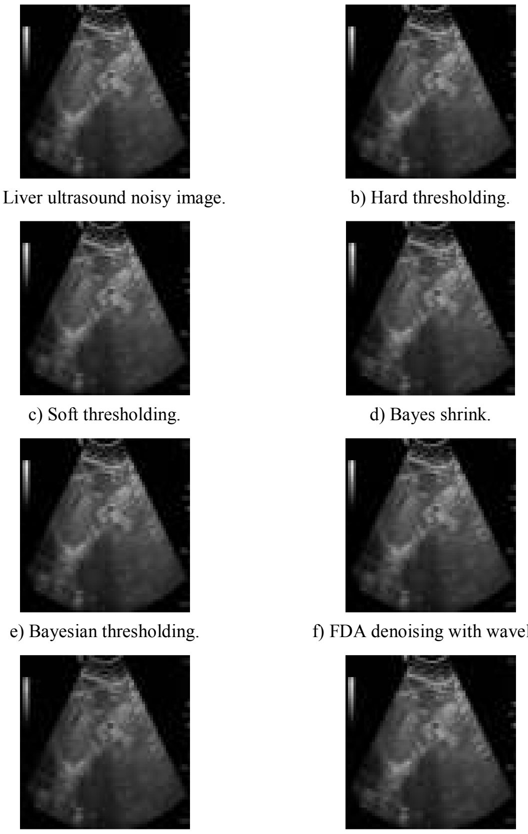

a) Liver ultrasound noisy image. b) Hard thresholding.

c) Soft thresholding. d) Bayes shrink.

e) Bayesian thresholding. f) FDA denoising with wavelet.

g) Filtered BIMF (10 levels). h) FDA denoising with BEMD.

Figure 8. Visual comparison of Liver ultrasound image after execution some existing state-of-the-art filters and our proposed filter on Liver ultrasound noisy image.

8. Conclusions

We have proposed an effective method for speckle BEMD using FDA proposed optimal threshold value. Our method exhibits better performance in comparison to existing methods for speckle noise reduction, edge preservation, visual quality and mean squared error. Our investigated method is especially effective for inhomogeneous image and can be used widely for speckle noise suppression of speckle affected images.

References

[1] Achim A., Bezeriano A., and Tasakalides P., "Novel Bayesian Multiscale for Speckle Removal in Medical Ultrasound Images," *IEEE Transactions on Medical Imaging Journal*, vol. 20, no. 8, pp. 772-783, 2001.

[2] Azim G. and Abo-Eleneen Z., "Thresholding Based on Fisher Linear Discriminant," *the Journal of Pattern Recognition Research*, vol. 6, no. 2, pp. 326-334, 2011.

[3] Cheney W. and Kincaid D., *Numerical Mathematics and Computing*, Brooks/Cole, 1999.

[4] Damerval C., Meignen S., and Perrier V., "A Fast Algorithm for Bidimensional EMD," *IEEE Signal Processing Letters*, vol. 12, no. 10, pp. 701-704, 2005.

[5] Donoho D. and Johnstone I., "Adapting to Unknown Smoothness via Wavelet Shrinkage," *Journal of the American Statistical Association*, vol. 90, no. 432, pp. 1200-1224, 1995.

[6] Donoho D. and Johnstone I., "Ideal Spatial Adaptation via Wavelet Shrinkage," *Biometrica*, vol. 81, no. 3, pp. 425-455, 1994.

[7] Donoho D. and Johnstone I., "Wavelet Shrinkage: Asymptopia," *Journal of the Royal Statistical Society*, vol. 57, no. 2, pp. 301-369, 1995.

[8] Fodor I. and Kamath C., "Denoising Through Wavelet Shrinkage: An Emperical Study," *Journal of Electronic Imaging*, vol. 12, no. 1, pp. 151-160, 2003.

[9] Grace C., Yu B., and Vattereli M., "Adaptive Wavelet Thresholding for Image Denoising and Compression," *IEEE Transaction*, *Image Processing*, vol. 9, no. 9, pp. 1532-1546, 2000.

[10] Grace C., Yu B., and Vattereli M., "Spatially Adaptive Wavelet Thresholding with Context Modeling for Image Denoising," *IEEE Transaction*, *Image Processing*, vol. 9, no. 9, pp. 1522-1530, 2000.

[11] Grace C., Yu B., and Vattereli M., "Wavelet Thresholding for Multiple Noisy Image Copies," *IEEE Transaction*, *Image Processing*, vol. 9, no. 9, pp. 1631-1635, 2000.

[12] Huang N., Shen Z., Long S., Wu M., Shih H., Zheng Q., Yen N., Tung C., and Liu H., "The Empirical Mode Decomposition and the Hilbert Spectrum for Non-Linear and Non-Stationary Time Series Analysis," *Proceedings of Royal Society of London A*, vol. 454, no. 1971, pp. 903-995, 1998.

[13] Jansen M., *Noise Reduction by Wavelet Thresholding*, Springer-Verlag New York Inc, 2001.

[14] Linderhed A., "2D Empirical Mode Decompositions in the Spirit of Image Compression," *in Proceedings of SPIE*, Arizona, USA, pp. 1-8, 2002.

[15] Muhsen Z., Dababneh M., and Nsour A., "Wavelet and Optimal Requantization Methodology for Lossy Fingerprint Compression," *the International Arab Journal of Information Technology*, vol. 8, no. 4, pp. 383-387, 2011.

[16] Nunes J., Bouaoune Y., Delechelle E., Niang O., and Bunel P., "Image Analysis by Bidimensional Empirical Mode Decomposition," *Image and Vision Computing*, vol. 21, no. 12, pp. 1019-1026, 2003.

[17] Otsu N., "A Threshold Selection Method from Gray-Level Histograms," *IEEE Transaction on Systems*, *Man and Cybernetics*, vol. 9, no. 1, pp. 62-66, 1979.

[18] Rahman M., PK M., and Uddin M., "Optimum Threshold Parameter Estimation of Wavelet Coefficients using Fisher Discriminant Analysis for Speckle Noise Reduction," *the International Arab Journal of Information Technology*, vol. 11, no. 6, pp. 573-581, 2014.

[19] Rajan J. and Kaimal M., "Image Denoising using Wavelet Embedded Anisotropic Diffusion (WEAD)," *in Proceedings of International Conference on Visual Information Engineering*, Bangalore, India, pp. 589-593, 2006.

[20] Sattar F., Floreby L., Salomonsson G., and Lovstorm B., "Image Enhancement based on a Nonlinear Multiscale Method," *IEEE Transactions*, *Image processing*, vol. 6, no. 6, pp. 888-895, 1997.

[21] Shaho B., Wang Y., Deng X., and Wang S., "Sparse Linear Discriminant Analysis by Thresholding High Dimensional Data," *the Annals of statistics*, vol. 39, no. 2, pp. 1241-1265, 2011.

[22] Vattereli M. and Kovacevic J., *Wavelets and Subband Coding*, Prentice Hall, 1995.

[23] Wang W., "Time-Frequency Analyses and Their Fast Implementation Algorithm," *Master Thesis*, National Taiwan University, 2009.

[24] Wu H. and Huang D., "Kernel Fisher Discriminant Analysis using Feature Vector Selection for Fault Diagnosis," *in Proceedings of the 2nd International Symposium on Intelligent Information Technology Application*, Shanghai, China, pp.109-113, 2008.

Mohammad-Motiur Rahman received the BSc Engineering and MS degrees in computer science and engineering from Jahangirnagar University, Bangladesh, in 1995 and 2001. Currently, he is pursuing the PhD degree. His research interests include: Digital image processing, medical image processing, computer vision and digital electronics. He has many International Journal and Conference Publications.

Mithun-Kumar Pk received the BSc engineering degree in computer science and engineering from Mawlana Bhashani Science and Technology University, Bangladesh. His research interests include: Image analysis, image processing and medical image processing, pattern recognition, 3D visualization, segmentation, filter optimization. He has many International Journal and Conference publications and he is a regular reviewer of IET Image Processing Journal.

Mohammad-Shorif Uddin is currently working in Department of Computer Science and Engineering, Jahangirnagar University, Bangladesh. His research is focused on bioimaging and image analysis, computer vision, pattern recognition, blind navigation, medical diagnosis and disaster prevention. He published many papers in renowned journals like IEEE, Elsevier, Iet, Optical Society of America etc.